Applied Stochastic Analysis Final Project:

Kinetic Monte Carlo (KMC) Simulations on Falicov-Kimball Model

Christine Wu (email:cw4459@nyu.edu)

May 8 2024

Abstract

This documentation illustrates the study on the paper *Anomalous phase separation in a correlated electron system: Machine-learning–enabled large-scale kinetic Monte Carlo simulations* (▷ https://www.pnas.org/doi/epdf/10.1073/pnas.2119957119)[**1**], and its connections with applied stochastic processes. In the paper, the authors investigate the dynamics of phase separation in correlated electron systems, a fundamental phenomenon in condensed matter physics with implications for material properties. Utilizing stochastic analysis techniques, specifically large-scale kinetic Monte Carlo simulations, they explore the phase-ordering processes in the Falicov-Kimball model, a canonical model for strongly correlated electron systems. In their findings, they uncover complex, multi-scale dynamics including unusual relaxation behaviors and spatial pattern formations like checkerboard and superclusters, providing new insights into the mechanisms driving phase separation in non-equilibrium electron systems. Here, we implemented a similar method (Kinetic Monte Carlo (kMC) simulations) and reproduced a few figures from the paper with some variations. In addition, we also provided some extra insights, in terms of the system change with temperature variations and different materials properties. There are also two interesting movies generated. Moreover, Hamiltonian Monte Carlo (HMC) and Quantum Monte Carlo (QMC) were also briefly mentioned.

1 Mathematical Background

1.1 Kinetic Monte Carlo (kMC) simulations

Kinetic Monte Carlo (KMC) can be seen as an extension of the Metropolis class of algorithms, which are designed to sample from a complex target probability distribution. Denote $\boldsymbol{\pi}$ as the target probability distribution, and $\mathbf{P}$ as the transition matrix of the corresponding Markov chain. Then we have $\boldsymbol{\pi}\mathbf{P} = \boldsymbol{\pi}$. This means that $\boldsymbol{\pi}$ is a stationary distribution of the Markov chain, which ensures that the chain, if run indefinitely, converges to $\boldsymbol{\pi}$. A fundamental aspect of Monte Carlo methods is to approximate integrals using the law of large numbers. Specifically, we aim for the empirical mean of a function f evaluated at the states of the Markov chain to converge to the expected value under $\boldsymbol{\pi}$, formally given by:

$$\frac{1}{N}\sum_{k=1}^{N} f(X^k) \to \int f(x)\pi(dx) \quad \text{as } N \to \infty \tag{1}$$

In order to achieve this goal, we can use Metropolis-Hastings Algorithm.

Definition 1.1 (Metropolis-Hastings Algorithm)**.** The Metropolis-Hastings Algorithm involves selecting a transition density $q(y|x)$. The algorithm operates under two scenarios:

1. If $\int q(y \mid x)\pi(dx) = \pi(y)$, then the transition density q is said to preserve π, maintaining the target distribution π unchanged.
2. Otherwise, the algorithm proceeds with generating a new state in the following manner:
   - Generate $Y^{k+1} \sim q(y \mid X^{(k)})$, where Y^{k+1} is the proposed next state in the Markov chain from the current state $X^{(k)}$.

- Accept Y^{k+1} as the new state X^{k+1} with the acceptance probability:

$$\text{pacc} = \min\left\{1, \frac{\pi(Y^{(k+1)})q(X^{(k)} \mid Y^{(k+1)})}{\pi(X^{(k)})q(Y^{(k+1)} \mid X^{(k)})}\right\} \tag{2}$$

If not accepted, set $X^{(k+1)} = X^{(k)}$. Otherwise, set $X^{(k+1)} = Y^{(k+1)}$.

▷▷ **Detailed Balance in Metropolis-Hastings Algorithm**

The detailed balance condition can be demonstrated for the Metropolis-Hastings (M-H) algorithm as follows:

$$q(y \mid x)\text{pacc}(x, y)\pi(x) = q(y \mid x)\min\left\{1, \frac{\pi(y)q(x \mid y)}{\pi(x)q(y \mid x)}\right\}\pi(x) \tag{3}$$

$$= \min\{q(y \mid x)\pi(x), \pi(y)q(x \mid y)\} \tag{4}$$

$$= q(x \mid y)\text{pacc}(y \mid x)\pi(y) \tag{5}$$

This ensures that q is in detailed balance with the stationary distribution π.

▷▷ **Transition Operation**

Consider the transition operation T defined as:

$$Tf(x) = \mathbb{E}[f(X^{(1)} \mid X^{(0)} = x)] \tag{6}$$

$$= f(x)P_{\text{rej}}(x) + \int f(y)\text{pacc}(x, y)q(y \mid x)\, dy \tag{7}$$

where $P_{\text{rej}}(x) = \int(1 - \text{pacc}(x, z))q(z \mid x)\, dz$. The transition probability density $p(y \mid x)$ is then:

$$p(y \mid x) = \delta(y - x)P_{\text{rej}}(x) + \text{pacc}(x, y)q(y \mid x) \tag{8}$$

and the operation T can be expressed as:

$$Tf(x) = \int f(y)p(y \mid x)\, dx \tag{9}$$

▷▷ **Validation of Detailed Balance via Transition Operator**

Detailed balance in terms of the transition operator requires that:

$$\int q(x)Tf(x)\pi(dx) = \int f(x)Tg(x)\pi(dx), \quad \forall g, f \tag{10}$$

This is verified as follows:

$$\int g(x)Tf(x)\pi(dx) = \int g(x)f(x)P_{\text{rej}}(x)\pi(dx) + \iint f(y)q(y \mid x)\text{pacc}(x, y)g(x)\pi(x)\, dx\, dy \tag{11}$$

$$= \int f(y)\int g(x)q(x \mid y)\text{pacc}(y, x)\, dx\pi(y)\, dy \tag{12}$$

$$= \int f(x)Tg(x)\pi(dx) \tag{13}$$

▷▷ **Choice of Transition Density** $q(y \mid x)$

For the transition density $q(y \mid x)$, we can consider a Gaussian proposal:

$$q(y \mid x) = \frac{e^{-(y-x)^2/2\sigma^2}}{\sqrt{2\pi\sigma^2}} = q(x \mid y) \tag{14}$$

where $y = x + N(0, \sigma^2)$, or alternatively, define $q(y \mid x)$ in a manner consistent with the energy levels of a transition state in a physical system, potentially expressed in a Hamiltonian formulation.

1.2 Hamiltonian Monte Carlo (HMC) simulations

Hamiltonian Monte Carlo (HMC) uses Hamiltonian dynamics to propose transitions in a Markov chain. The Hamiltonian $H(x, p)$, combining potential energy $U(x)$ and kinetic energy $K(p)$, governs the dynamics. The transition density in HMC is derived from simulating the trajectory under Hamilton's equations:

$$\frac{dx}{dt} = \frac{\partial H}{\partial p}, \qquad \frac{dp}{dt} = -\frac{\partial H}{\partial x} \tag{15}$$

The acceptance of transitions is based on the change in the Hamiltonian:

$$\text{Acceptance Probability} = \min\left(1, e^{-[H(x',p')-H(x,p)]}\right) \tag{16}$$

where (x, p) is the current state and (x', p') is the proposed state **[2]**. As we know, any physical systems can be presented in terms of kinetic and potential energies in a form of a Hamiltonian, but there is a transition between a classical system and quantum system, which relates to the potential energy level.

1.3 Quantum Monte Carlo (QMC) simulations

▷▷ Calculation of Chemical Potential

The chemical potential μ in a semiconductor can be estimated by solving the electron density equation:

$$n = \int_0^\infty D(E) \left(\frac{1}{e^{(E-\mu)/k_B T} + 1}\right) dE \tag{17}$$

where $D(E)$ is the density of states, K_B is the Boltzmann constant and T is the temperature.

Given specific values for n, $D(E)$, T, and assuming a particular form for $D(E)$, we would typically use numerical methods to solve for μ. This involves iterative techniques to find μ such that the total number of electrons matches the expected electron density.

▷▷ Integration of Fermi-Dirac Statistics in Quantum Monte Carlo Simulations

Quantum Monte Carlo (QMC) methods are essential for addressing complex quantum systems. They are particularly useful in simulations of fermionic systems, such as electrons, where Fermi-Dirac statistics and the Pauli exclusion principle play critical roles. During simulations, the chemical potential μ is adjusted to maintain the correct particle density, utilizing the Fermi-Dirac distribution within the Metropolis algorithm to manage state transition probabilities **[3]**. In this documentation, we are specifically interested in one quantum system - Falicov-Kimball Model.

1.4 Falicov-Kimball Model

▷▷ The basic model

The spinless Falicov-Kimball model (as mentioned in the paper) is crucial in condensed matter physics for studying interactions between localized and itinerant electron species. It features a Hamiltonian:

$$H = -t_{\text{nn}} \sum_{\langle i,j \rangle} (c_i^\dagger c_j + c_j^\dagger c_i) + U \sum_i n_i^c n_i^f \tag{18}$$

where $c_i^\dagger$ and c_i are the creation and annihilation operators for itinerant c-electrons at each lattice site i. The model sums over nearest-neighbor pairs $\langle i, j \rangle$ to reflect spatial interactions through hopping, with $n_i^c = c_i^\dagger c_i$ and n_i^f representing the number operators for itinerant and localized electrons, respectively. The Hamiltonian incorporates t_{nn} as the hopping constant and energy unit for kinetic movements, and U for the Coulomb interaction between itinerant and localized electrons at the same site.

▷▷ Dynamics of Electron Movement

The motion of localized f-electrons is influenced by the quasi-equilibrium states of itinerant c-electrons. Updates in the configuration, especially moves between nearest-neighbor sites, are governed by the acceptance probability:

$$p_{i \to j} = \min\left(1, e^{-\Delta E_{i \to j}/k_B T}\right) \tag{19}$$

Here, $\Delta E_{i \to j}$ is the energy change, with k_B as the Boltzmann constant and T the system temperature. This setup promotes energy minimization, aligning with the principles of statistical mechanics **[1]**.

2 Simulation Integration

In the paper [**1**], the authors used machine learning-enabled large-scale kinetic Monte Carlo (KMC) simulations to study the Falicov-Kimball model. Due to the lack of the original training data sets from the paper for the machine-learning purpose, we will focus on the simulations more on kinetic Monte Carlo (KMC) solely. However, we decided to incorporate some new thoughts on the topic, which was not mentioned in the paper, including the temperature investigation, as well as the correlation between the effective potential and the cluster formation.

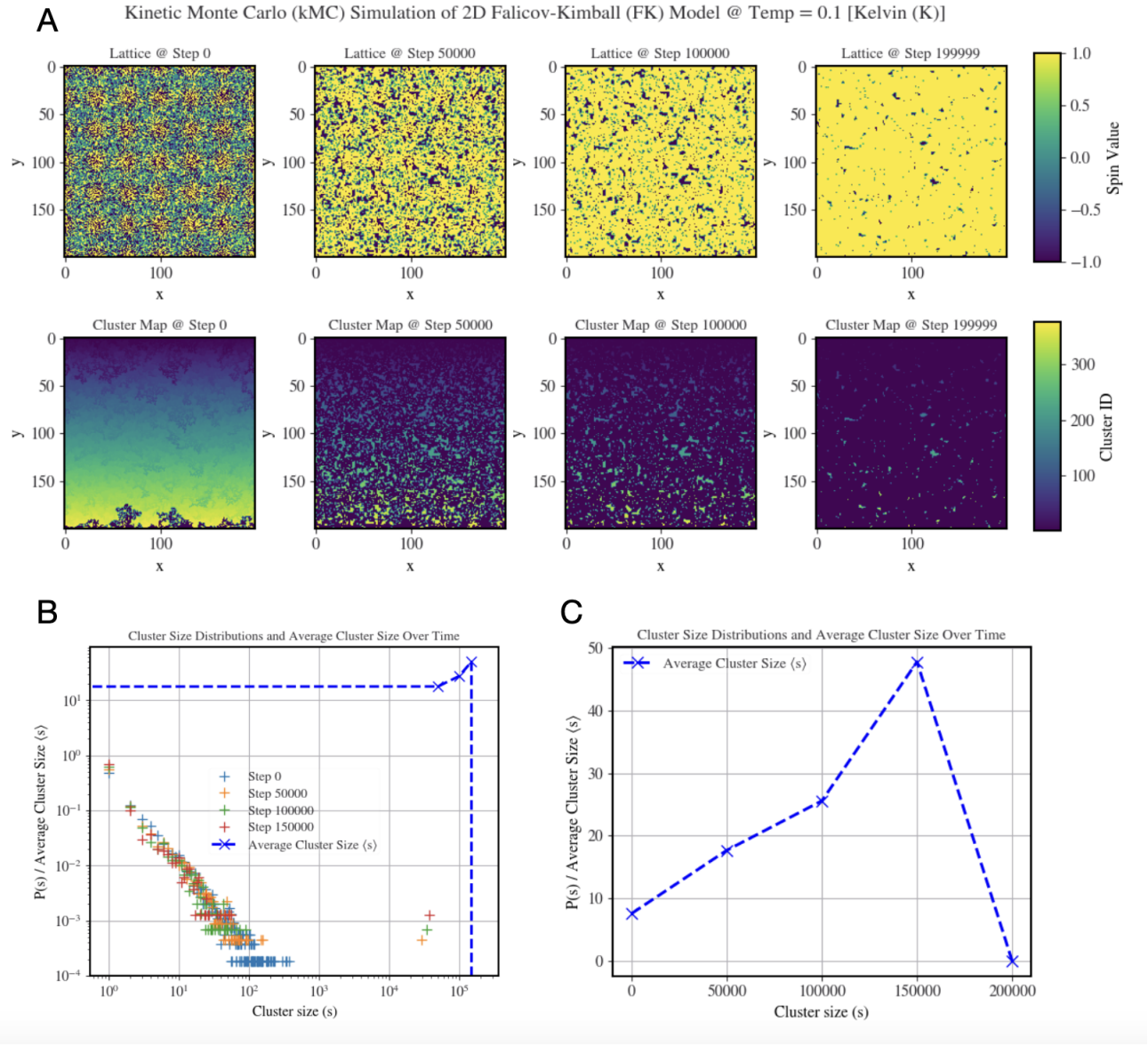

Figure 1: Kinetic Monte Carlo (kMC) on Falicov-Kimball model at temperature @1K (Temperature in units where Boltzmann's constant kB = 1 (essentially scaling temperature). **A** describes the dynamics of the spin motions, migrating with the kMC steps on the first row, whereas on the second row, we have the dynamics of the cluster formation. **B** talks about the sizes and the probabilities of the cluster formations, with different kMC steps. **C** gives a better visualization of the probabilities of the growth of clusters with different sizes at the given conditions.

From the subplot **A**, on our 200×200 grid, as the kMC step progresses to our target which is $200,000$, we can see that the spin map moves towards a unified heterogeneous state, where every electron in our lattice, possibly has a spin up in their degenerate orbitals. According to Hund's rule, when the spins are parallel, we can achieve the most stable configuration results. On the second row of **A**, as the kMC step progresses, there is a phase-separation, where those checkerboard clusters described in the paper were formed. Subplots **B** and **C** describe the sizes and the probability growth of those clusters, and how it correlates with the time steps. From **B**, we noticed that after step $50,000$, we started to have super-clusters formed, which is between the size of 10^4 and 10^5, where the most occurred size of the super-cluster is around $1.5 * 10^5$ as **C** indicates. Furthermore, in order to understand the system more, as trained in science, we know that temperature is a key factor that affects any physical systems. So, it will be the next.

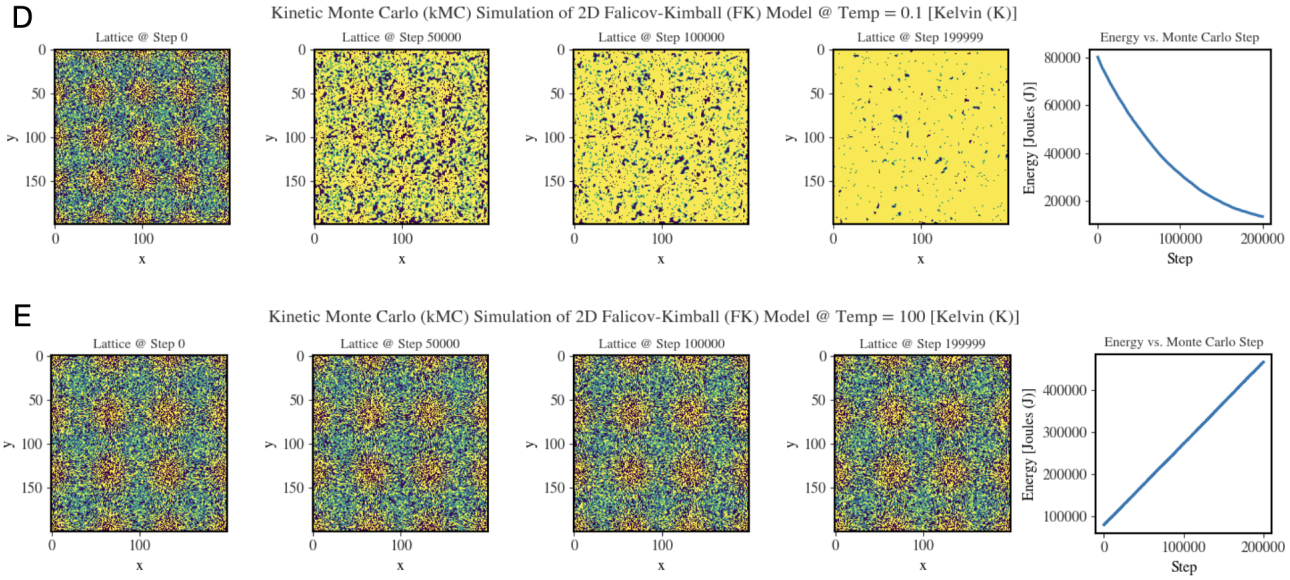

Figure 2: Kinetic Monte Carlo (kMC) on the Falicov-Kimball model at different temperatures and its correlation with energy levels. **D** tells the story of the dynamics at temp = 0.1K, and **E** does the same thing with temp = 100K.

The dynamics are different when we have different temperatures but everything else is the same. **D**, as we discussed in Figure 1, we know such conditions will support clusters forming properly. The corresponding energy also decreases as the step moves forward for a more stabilized state. This is because the spin co-alignment usually forms at low or moderate temperatures to achieve proper quantum interactions. However, **E**, on the other hand, does not achieve the stable state, and the energy keeps increasing to indicate a randomized system, interfered with by high temperature. This increase in energy is indicative of the thermal agitation overpowering the spin interaction energies, preventing the formation of stable clusters or aligned domains. In such high-temperature scenarios, the lattice remains in a dynamic state with frequent spin flips and little to no long-term order. This behavior underscores the disruptive impact of high thermal energy on the quantum mechanical interactions that typically help stabilize the system. This phenomenon can also be observed from the correlation between the lattice dynamics and the potential changes.

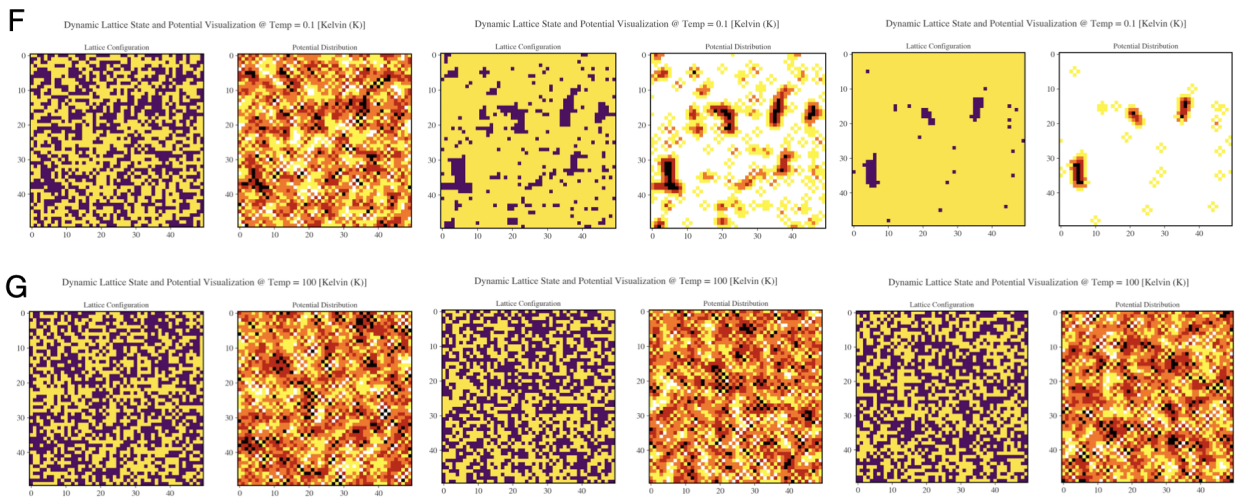

Figure 3: Movie screenshots for the comparison between the lattice dynamics and the effective potential changes at different temperature for a grid size of 50×50. **F** tells the story of the dynamics at temp $= 0.1$K, and **G** does the same thing with temp $= 100$K.

As we can tell, there is a strong correlation between the lattice dynamics (the checkboard cluster domains) and the effective potential energy changes. Because of such, as described in the paper, f electrons in the neighborhood thus tend to reside on the same sublattice, leading to the growth of the supercluster. As time propagates, they grow bigger and bigger and eventually occupy the whole lattice, creating a stable and orderly state. However, that does not imply the case at higher temperatures, the whole system will keep changing, since it is in the unstable state as previously discussed. The details of the movies can be found on the Github site provided in the conclusion section.

3 Conclusions

In this document, we briefly illustrated a simple Kinetic Monte Carlo (kMC) on the Falicov-Kimball model, based on the paper mentioned at the beginning. We understand now that at a relatively low temperature, the spin system can give non-equilibrium phase-separation dynamics, where the energy will be lowered, and checkerboard clusters can form to give materials proper insulation properties. In terms of the simulations, they were all done using Python, where the code can be found at https://github.com/cw0508/asa_final_project. However, all the calculations presented here are simplified, where we keep the Boltzmann's constant as 1, where it is supposed to be 1.38×10^{-23}J/K in reality and the hopping constant t_{nn} as 1 and the coulomb interaction U as 2, where they should be varied according to different materials due to different material properties. Although a general model is presented here, we should keep in mind that its derivations are from real physical systems from a case-to-case scenario.

▷▷ **Some useful links to check for possible future work:**

- The general Falicov-Kimball model: https://arxiv.org/pdf/math-ph/0502041
- Exact solution of the Falicov-Kimball model with dynamical mean-field theory (with some real materials investigations): https://arxiv.org/pdf/math-ph/0502041
- The materials project (to see different materials properties): https://next-gen.materialsproject.org
- The Staggered Mesh Method or Fock exchange energy in periodic lattice systems (with some real materials investigations): https://arxiv.org/pdf/2402.13538v1

References

[1] Zhang, S., Zhang, P., & Chern, G. (2022). Anomalous phase separation in a correlated electron system: Machine-learning–enabled large-scale kinetic Monte Carlo simulations. *Proceedings of the National Academy of Sciences of the United States of America*, 119(18). https://doi.org/10.1073/pnas.2119957119

[2] Team, S. D. (n.d.). 14.1 Hamiltonian Monte Carlo — StAN Reference Manual. https://mc-stan.org/docs/2_19/reference-manual/hamiltonian-monte-carlo.html

[3] Wikipedia contributors. (2024, April 30). Hamiltonian Monte Carlo. Wikipedia. https://en.wikipedia.org/wiki/Hamiltonian_Monte_Carlo